Enhanced Quadrupole Effects for Atoms in Optical Vortices

V. E. Lembessis[1] and M. Babiker[2]

[1]*Department of Physics and Astronomy, College of Science, King Saud University, Riyadh 11451, Saudi Arabia*
[2]*Department of Physics, University of York, Heslington, York YO10 5DD, United Kingdom*
(Received 2 October 2012; published 21 February 2013)

We show that the normally weak optical quadrupole interaction in atoms is enhanced significantly when the atom interacts at near resonance with an optical vortex. In particular, the forces and torque acting on the atom are shown here to scale up with the square of the winding number l of the vortex. Because the integer l can be arranged to be large, this property allows for processes involving dipole-forbidden, but quadrupole-allowed, transitions in atoms, such as cesium and oxygen, to come into play. We show that the mechanical effects of vortex light on atoms involving translational and rotational motion as well as trapping should be significantly enhanced for quadrupole transitions and present novel features with useful implications for the emerging field of atomtronics.

It is common scientific knowledge that photon processes involving the interaction of atoms and molecules with lasers are dominated by dipole-active transitions. Higher multipolar effects are normally considered to be too small for consideration in the contexts of most experimental scenarios [1]. The next in the multipolar order is the electric quadrupole. However, when compared with electric dipole transitions, the electric quadrupole transition rates are typically smaller by a factor $\alpha = (a_0 k)^2$, where a_0 is the Bohr radius and k is the wave number of the ordinary laser light. For processes involving transitions in the optical region we have $\alpha \approx 10^{-6}$.

Optical measurement techniques have advanced significantly in recent years and quadrupole transitions can now be observed and utilized [2,3]. Other recent studies have been concerned with the enhancement of quadrupole effects in the vicinity of material surfaces, including microstructures where enhancements by 2 orders of magnitude are predicted and have been experimentally observed [4–6]. To date, and as far as the authors are aware, quadrupole effects have not featured in investigations concerned with the mechanical effects of laser radiation on atoms because of the dominance of electric dipole-active transitions. Investigations of the mechanical effects of laser light on atoms have led to a number of important applications, including trapping and cooling of atoms, atom optics, the creation of atomic Bose-Einstein condensates, atom lasers, atoms in optical lattices, and quantum simulators [7–9]. As in mainstream atom-optical investigations, the common feature has so far been the interaction of nearly resonant laser beams with atoms, which can be modeled, to a good approximation, as two-level systems in which the interaction with the laser light involves dipole-active transitions between the two atomic levels [10–12].

One of the main developments in atom-field interactions over the last two decades or so is the advent of vortex laser beams that are characterized by the property of quantized orbital angular momentum [13–17]. The mechanical effects of vortex laser light on atoms have formed a subject of considerable interest, both in theory and experiment. Each photon of a vortex beam imparts a momentum as well as an angular momentum to an atom. The photon angular momentum, which is quantized, is responsible for the appearance on the atoms of a torque that strongly affects their rotational motion. The effects of the torque on atomic cooling and trapping of atoms have been studied in a number of contexts [18–26], but only for dipole-active transitions.

Here we carefully analyze quadrupole effects in the interaction of atoms with optical vortices. The aim is to explore the spatial dependence of the quadrupole Rabi frequency and its magnitude relative to the case with ordinary light, how this is influenced by the vorticity of the light, and the consequences of this on the atom trapping and atom dynamics due to the forces and torque acting on the atom in the field of the optical vortex.

The physical system consists of the atom, modeled here as a neutral two-particle hydrogenic atom possessing only two energy levels, a ground state, denoted $|1\rangle$ of energy $\mathcal{E}_1$, and an excited state $|2\rangle$ of energy $\mathcal{E}_2$, such that the resonance frequency is $\omega_0 = (\mathcal{E}_2 - \mathcal{E}_1)/\hbar$. The atom interacts with the optical vortex in the form of a Laguerre-Gaussian (LG) mode characterized by the quantum numbers l and p propagating along the z axis with an axial wave vector k. The total Hamiltonian is

$$\hat{H} = \hat{H}_A + \hat{H}_F + \hat{H}_{\text{int}}, \qquad (1)$$

where $\hat{H}_A$ and $\hat{H}_F$ are the zero-order Hamiltonians for the atom and the LG field, respectively,

$$\hat{H}_A = \frac{\mathbf{P}^2}{2M} + \hbar\omega_0 \pi^\dagger \pi, \qquad (2)$$

$$\hat{H}_F = \hbar\omega a_{klp}^\dagger a_{klp}. \qquad (3)$$

Here **P** is the center-of-mass momentum operator and π and $\pi^\dagger$ are the atomic level lowering and raising operators; M is the mass of the atom. In Eq. (3), a_{klp} and $a_{klp}^\dagger$ are the LG mode annihilation and creation operators and ω is the frequency of the field. The interaction Hamiltonian involves the coupling of the electric polarization $\mathcal{P}(\mathbf{r})$ to the LG electric field vector, as follows:

$$\hat{H}_{\text{int}} = -\int d^3 r \, \mathcal{P}(\mathbf{r}) \cdot \mathbf{E}(\mathbf{r}). \qquad (4)$$

The explicit form of the polarization field $\mathcal{P}$ is [1]

$$\mathcal{P}(\mathbf{r}) = e \int_0^1 ds (\mathbf{q} - \mathbf{R}) \delta(\mathbf{r} - \mathbf{R} - s(\mathbf{q} - \mathbf{R})), \qquad (5)$$

where $\mathbf{R}$ is the center-of-mass coordinate and $(\mathbf{q} - \mathbf{R})$ is the internal position variable relative to the center of mass. Expansion of the polarization field $\mathcal{P}$ in a multipolar series about the center of mass $\mathbf{R}$ followed by integration with respect to $\mathbf{r}$, yields up to quadrupolar order,

$$\hat{H}_{\text{int}} = \hat{H}_d + \hat{H}_{\text{QE}} + \cdots, \qquad (6)$$

where $\hat{H}_d$ is the coupling of field to the electric dipole moment and $\hat{H}_{\text{QE}}$ is the coupling to the electric quadrupole moment. Explicitly we have

$$\hat{H}_d = -\mathbf{d} \cdot \mathbf{E}(\mathbf{R}), \qquad (7)$$

where $\mathbf{d} = e\mathbf{x}$ is the electric dipole moment operator with $\mathbf{x} = (\mathbf{q} - \mathbf{R})$. The quadrupole term is then explicitly given by

$$\hat{H}_Q = -\tfrac{1}{2} e x_i x_j \nabla_i E_j(\mathbf{R}), \qquad (8)$$

where the Einstein summation convention is applicable. Here x_i are the components of the internal position vector $\mathbf{x} = (x, y, z)$ and ∇_j are components of the gradient operator that act only on the spatial coordinate of the transverse electric field vector $\mathbf{E}$ as function of the center-of-mass variable $\mathbf{R}$.

The Laguerre-Gaussian mode is assumed to be linearly polarized along the x direction such that its quantized electric field as a function of the center-of-mass coordinate $\mathbf{R} = (X, Y, Z)$ now expressed in cylindrical coordinates $\mathbf{R} = (r, \phi, Z)$ has the form

$$\mathbf{E}(\mathbf{R}) = \hat{\boldsymbol{i}} E_{k00} u_p^{|l|}(r) \hat{a}_{klp} e^{i\Theta_{klp}(\mathbf{R})} + \text{H.c.}, \qquad (9)$$

where $u_p^{|l|}(r)$ is given by

$$u_p^{|l|}(r) = C_{pl} \left[\frac{r\sqrt{2}}{w_0} \right]^{|l|} L_p^{|l|}\left(\frac{2r^2}{w_0^2} \right) e^{-r^2/w_0^2}, \qquad (10)$$

where $C_{pl} = \sqrt{p!/(|l| + p)!}$ is the normalization constant of the Laguerre-Gaussian function. Θ is the phase of the mode

$$\Theta_{klp}(\mathbf{R}) = kZ + l\phi. \qquad (11)$$

Here L_p^l is the Laguerre polynomial and w_0 is the radius at beam waist at $Z = 0$; E_{k00} is the constant amplitude of a plane wave of the same intensity and a_{klp} is the annihilation operator for the field mode, while H.c. stands for Hermitian conjugate. In order not to obscure the main purpose of this investigation by avoiding cluttered formalism, we have assumed that the LG mode has a long Rayleigh range and we ignore all mode curvature effects.

The forces and trapping potential due to the dipole interaction equation (7) with the vortex field defined by Eqs. (9) to (11) have been extensively analyzed [17,25,26].

With the electric field polarized along the x direction, designated by the appearance of the unit vector $\hat{\boldsymbol{i}}$ in Eq. (9), the quadrupole interaction Hamiltonian equation (8) now takes the form

$$\hat{H}_Q = \frac{1}{2}\left\{ \hat{Q}_{xx}\frac{\partial E_x}{\partial X} + \hat{Q}_{xy}\frac{\partial E_x}{\partial Y} + \hat{Q}_{xz}\frac{\partial E_x}{\partial Z} \right\}, \qquad (12)$$

where $\hat{Q}_{ij} = -ex_i x_j$ are the elements of the quadrupole tensor operator, which for the two-level atom can be written as

$$\hat{Q}_{ij} = Q_{ij}(\pi + \pi^\dagger), \qquad (13)$$

where $Q_{ij} = \langle 1|\hat{Q}_{ij}|2\rangle$ are quadrupole matrix elements between the two atomic levels.

Substituting from Eq. (9) in Eq. (12) we can write the quadrupole interaction Hamiltonian in the form

$$\hat{H}_Q = \hbar \hat{a}_{klp} \Omega_{klp}^Q(\mathbf{R}) e^{i\Theta_{klp}(\mathbf{R})} + \text{H.c.} \qquad (14)$$

Here $\Omega_{klp}^Q(\mathbf{R})$ is the complex Rabi frequency defined as follows:

$$\hbar\Omega_{klp}^Q(\mathbf{R}) = E_{k00} u_p^l(\mathbf{R})\{Q_{xx}\mathcal{F} + Q_{yx}\mathcal{J} + ikQ_{zx}\}, \qquad (15)$$

where

$$\mathcal{F} = \left(\frac{|l|X}{r^2} - \frac{2X}{w_0^2} - \frac{ilY}{r^2} + \frac{1}{L_p^{|l|}}\frac{\partial L_p^{|l|}}{\partial X} \right);$$

$$\mathcal{J} = \left(\frac{|l|Y}{r^2} - \frac{2Y}{w_0^2} + \frac{ilX}{r^2} + \frac{1}{L_p^{|l|}}\frac{\partial L_p^{|l|}}{\partial Y} \right). \qquad (16)$$

With both the phase and the complex Rabi frequency defined, the steady state force on the moving atom due to the LG laser mode is written

$$\langle \mathbf{F} \rangle_{klp}^Q = \langle \mathbf{F}_{\text{diss}}^Q \rangle_{klp} + \langle \mathbf{F}_{\text{quad}} \rangle_{klp}, \qquad (17)$$

where $\langle \mathbf{F}_{\text{diss}}^Q \rangle_{klp}$ is the dissipative force

$$\langle \mathbf{F}_{\text{diss}}^Q(\mathbf{R}, \mathbf{V}) \rangle_{klp}$$
$$= 2\hbar\Gamma|\Omega_{klp}^Q(\mathbf{R})|^2 \left(\frac{\boldsymbol{\nabla}\Theta_{klp}(\mathbf{R})}{\Delta_{klp}^2(\mathbf{R}, \mathbf{V}) + 2|\Omega_{klp}^Q|^2(\mathbf{R}) + \Gamma_Q^2} \right)$$
$$(18)$$

and $\langle \mathbf{F}_{\text{quad}} \rangle_{klp}$ is the quadrupole force

$$\langle \mathbf{F}_{\text{quad}}(\mathbf{R}, \mathbf{V}) \rangle_{klp} = -\hbar \boldsymbol{\nabla}(|\Omega^Q_{klp}|^2)$$
$$\times \left(\frac{\Delta_{klp}(\mathbf{R}, \mathbf{V})}{\Delta^2_{klp}(\mathbf{R}, \mathbf{V}) + 2|\Omega^Q_{klp}|^2(\mathbf{R}) + \Gamma^2_Q} \right), \tag{19}$$

where Γ_Q is the relaxation rate for the quadrupole spontaneous emission. The variable $\mathbf{R}(t)$ now denotes the position of the atom and $\mathbf{V} = \dot{\mathbf{R}}$ is the velocity, both at time t, while $\Delta_{klp}(\mathbf{R}, \mathbf{V})$ is the position- and velocity-dependent detuning,

$$\Delta_{klp}(\mathbf{R}, \mathbf{V}) = \Delta_0 - \mathbf{V} \cdot \boldsymbol{\nabla}\Theta_{klp}(\mathbf{R}, \mathbf{V}). \tag{20}$$

In these expressions Δ_0 is the static detuning defined by $\Delta_0 = \omega - \omega_0$. The dissipative force can now be understood as a quadrupole absorption followed by spontaneous emission of the light by the atom, while the quadrupole force, which is proportional to the gradient of the Rabi frequency, is responsible for confining the atom to the maximal intensity regions of the field, depending on the detuning Δ. The quadrupole force is derivable from a quadrupole potential

$$U_{\text{quad}}(\mathbf{R}) = -\frac{1}{2}\hbar\Delta \ln\left(1 + \frac{2|\Omega^Q_{klp}|^2(\mathbf{R})}{\Delta^2 + \Gamma^2_Q} \right). \tag{21}$$

In experimental situations where we have large detuning $|\Delta| \gg |\Omega^Q|$; $|\Delta| \gg \Gamma_Q$ the quadrupole potential can be written to a good approximation as follows:

$$U_{\text{quad}}(\mathbf{R}) \approx -\frac{\hbar}{\Delta}|\Omega^Q_{klp}|^2. \tag{22}$$

It is clear from the above expressions responsible for the steady state atomic motion that the modulus squared Rabi frequency $|\Omega^Q_{klp}(\mathbf{R})|$ is the key factor determining the dynamics of atoms in the field of the LG mode.

For illustration we will now consider the case of an LG doughnut mode of winding number l, but for which $p = 0$. In this case the derivative in $\mathcal{F}$ in Eq. (16) is equal to zero, because $L_0^{|l|}$ is a constant for all l. We shall also assume that the atom is constrained to move in the X-Y plane and the quadrupole transition is such that $Q_{xy} = 0 = Q_{xz}$. Under these circumstances the Rabi frequency Eq. (15) takes the following simpler form:

$$\hbar\Omega^Q_{kl0}(\mathbf{R}) = E_{k00}u_0^l(r)Q_{xx}\left(\frac{|l|X}{r^2} - \frac{2X}{w_0^2} - \frac{ilY}{r^2} \right). \tag{23}$$

Expressing lengths in units of w_0, so that $\bar{r} = r/w_0, \dots$, etc., we find for the modulus squared of the Rabi frequency entering the dissipative force in Eq. (18) and the quadrupole potential Eq. (22)

$$\hbar^2|\Omega^Q_{kl0}|^2 = E^2_{k00}|u_0^l|^2\left(\frac{Q_{xx}}{w_0} \right)^2 \left\{ \left(\frac{|l|\bar{X}}{\bar{r}^2} \right)^2 + \left(\frac{|l|\bar{Y}}{\bar{r}^2} \right)^2 \right.$$
$$\left. + 4\bar{X}^2\left[1 - \frac{|l|}{\bar{r}^2} \right] \right\}. \tag{24}$$

We now explore the spatial variations of the squared Rabi frequency given by Eq. (24) and the trapping potential given by Eq. (22) and how these are affected by the choice of the the vortex and atomic parameters. To be specific, we consider Cs as an atom recently explored for its quadrupolar transition $6^2S_{1/2} \rightarrow 5^2D_{5/2}$, specifying the deexcitation rate Γ_Q and a quadrupolar matrix element Q_{xx}. The optial vortex is such that the amplitude E_{000} is related to the intensity by $I = \epsilon_0 c E^2_{k00}/2$. We also need a suitable value for the detuning Δ and, since we wish to maximize the quadrupolar effects we take a large value of winding number l,

$$w_0 = \lambda/2; \qquad \lambda = 675 \text{ nm}; \qquad Q_{xx}10ea_0^2;$$
$$\Gamma_Q = 7.8 \times 10^5 \text{ s}^{-1}; \qquad \Delta_0 = 10^3\Gamma_Q; \qquad I = 10^9 \text{ W m}^{-2}. \tag{25}$$

It is also convenient to define a scaling parameter Ω_0 as follows:

$$\Omega_0 = \frac{1}{\hbar}\left(\frac{2I}{\epsilon_0 c} \right)^{1/2} \frac{Q_{xx}}{w_0} = 136\Gamma_Q, \tag{26}$$

where the last equality emerges on substituting the relevant parameters defined in Eq. (25).

The spatial distribution shown in Fig. 1(a) is the variation of the $|\Omega^Q_{kl0}|^2$ in units of Ω_0 for a doughnut vortex of winding number $l = 1$ and here we see the distribution peaking on the vortex core. It turns out that the appearance of a maximum variation at the vortex core is a preserve only of the case $l = 1$. Figure 1(b) on the other hand shows the corresponding variation of $|\Omega^Q_{kl0}|^2$ expressed in the same units when the winding number is increased to $l = 300$. Experimentally, winding numbers as large as $l = 300$ can be achieved, as emphasized recently [27]. The main features of the squared Rabi frequency plots can be explained by an analysis of Eq. (24) on substituting for $|u_p^{|l|}|^2$ from Eq. (10), expressed in terms of the dimensionless variables. In the large l case we have a distribution with two regions of variation and there are high symmetry points. To see dependence on l we consider the points $(\bar{X}, \bar{Y}) = (0, \pm 1)$, the expression between the curly brackets of the $|\Omega^Q_{kl0}|^2$ expression becomes equal to l^2, while at the points $(\bar{X}, \bar{Y}) = (\pm 1, 0)$ the curly bracket reduces to $(l - 2)^2$; both of these observations effectively scale as l^2 for large l. We have also verified that the maxima and zeros of $|\Omega^Q_{kl0}|^2$ actually occur at the following $(\bar{X}, \bar{Y})$ points:

$$(\bar{X}, \bar{Y}) = (\pm\sqrt{l/2}, 0)(\text{Minimum});$$
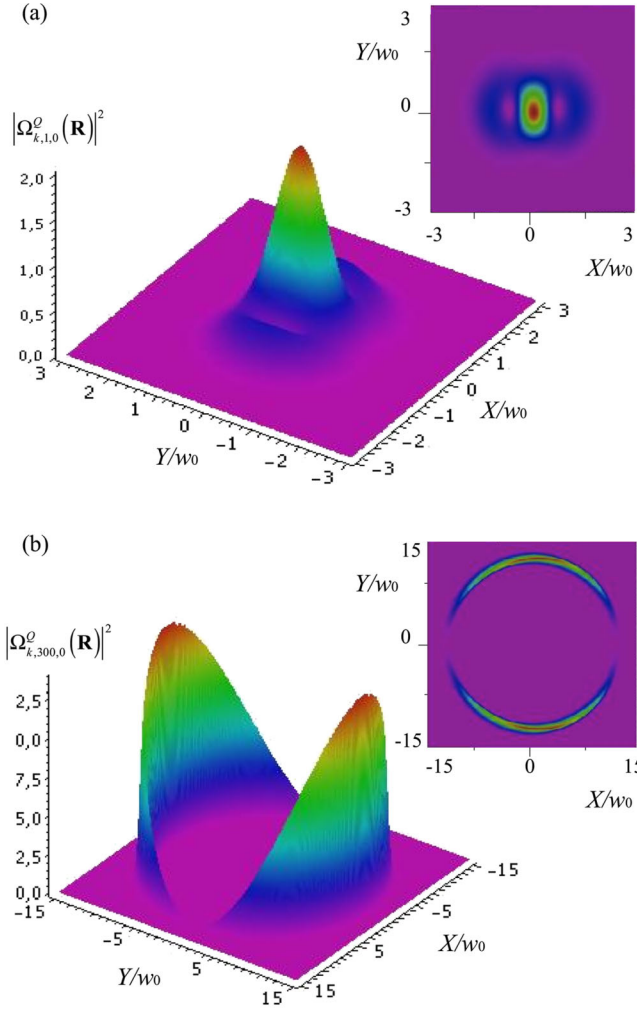$$(\bar{X}, \bar{Y}) = (0, \pm\sqrt{[l-1]/2})(\text{Maximum}). \tag{27}$$

(a)

(b)

FIG. 1 (color online). (a) The modulus squared Rabi frequency $|\Omega^Q_{klp}(\mathbf{R})|^2$, in units of Ω_0^2 defined in Eq. (26) for an atom in a Laguerre-Gaussian doughnut mode for which $l = 1$, $p = 0$. Distances are in units of w_0. (b) The large l case, $l = 300$, $p = 0$. The inset in each case shows the projections in the X-Y plane. The color code is such that from magenta to red is equivalent to from minimum to maximum. See the text for the parameters used to generate these figures and a discussion of the main features. The gray-scale color code is such that from dark gray (magenta) to light gray (red) is equivalent to from minimum to maximum.

These results hold even for the case $l = 1$; the maximum in that case occurs at the vortex core, as Fig. 1(a) shows.

Figure 2 shows the quadrupolar trapping potential for the set of parameters in Eq. (25) for the large $l = 300$. The depth of the this quadrupolar potential is seen to be of the following order:

$$U_{\min} \approx 1.25 \times 10^{-3} \text{ K,} \quad (28)$$

which is sufficiently deep to trap Cs atoms. We suggest that this result indicates that quadrupolar transitions normally ignored for atom dynamics should be available for exploitation.
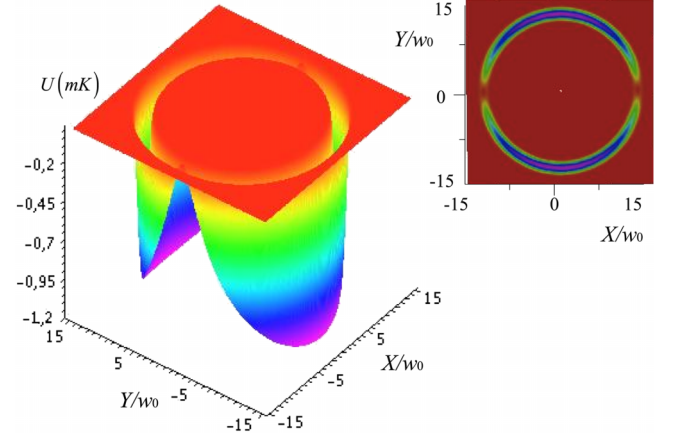

FIG. 2 (color online). The quadrupole optical potential distribution in millidegrees Kelvin (mK) for a doughnut mode with large l where $l = 300$, $p = 0$. The color code is the same as in Fig. 1; magenta now represents the lowest negative values of the quadrupolar trapping potential. The inset shows the projection in the X-Y plane. See the text for the parameters used to generate this plot and a discussion of the main features. The gray-scale color code is such that from dark gray (magenta) to light gray (red) is equivalent to from minimum to maximum.

In conclusion, our analysis has shown that the interaction of light endowed with orbital angular momentum can lead to significant mechanical effects on atoms characterized by a quadrupole-allowed transition. The form of the quadrupole Rabi frequency squared in the LG light indicates enhancements of both the dissipative force and the trapping potential in the processes involving quadrupolar transitions. Because it is relatively straightforward to generate LG light in the laboratory with large values of l [14,27], the quadrupolar mechanical effects should be amenable to experimental verification.

Recent experiments have succeeded in trapping cold sodium atoms in annular ringlike regions of space created by counter-propagating beams including twisted light [28] and the atoms were then made to rotate, generating a persistent current. This has been highlighted as paving the way for further developments in the emerging area of atomtronics [29–31]. We envisage that similar experiments could be designed in which atoms such as cesium and oxygen involving quadrupolar transitions are trapped in the quantum well regions of a large l LG mode. Trapping within the X-Y plane will require counter-propagating beams, as in the case of dipole transitions, in order to cool the axial motion to very small axial speed. The quadrupolar oxygen transition mentioned earlier is the well characterized $^1D_2 \rightarrow {}^1S_0$ quadrupolar transition of wavelength 557.73 nm. This is one of the green lines that dominate the aurora borealis spectrum under certain circumstances. In addition to Cs it would be interesting to trap oxygen using this quadrupole transition.

In the presence of external fields (e.g., static electric fields) a transition may be simultaneously both dipole and

quadrupole allowed. In that case if the conditions are such that quadrupole effects are significant, then they may be comparable or larger than the fluctuations of the forces corresponding to the dipole transition.

Other sources of enhancement of the quadrupole interaction in nonvortex contexts involve a combination of strong field gradients and high field intensity. It has been realized that this combination is easily achieved with the help of plasmonic nanostructures. This has been verified in cesium quadrupolar transitions, first when the atom interacts with the evanescent field due to total internal reflection [3] and, second, when it interacts with the field created around nanoantennas where the field is strongly confined and enhanced [4,5]. Excited atoms in the vicinity of nanostructures and undergoing spontaneous emission experience an enhanced rate of deexcitation. This is principally because the local density of states is increased near a plasmonic nanostructure and this leads to a drastic reduction of the excited state lifetime [4].

It then seems reasonable to suggest that a further enhancement source of quadrupolar vortex interactions could be by placing the atoms near the surface of plasmonic structures and arranging the generation of surface plasmonic modes endowed with the vortex properties. Dipole-allowed transitions are subject to strong enhancement under these conditions, as recent theoretical and experimental work have shown [32,33] and corresponding enhancements of quadrupolar effects are expected.

[1] C. Cohen-Tannoudji, *Atoms in Electromagnetic Fields* (World Scientific, Singapore, 1994); D. P. Craig and T. Thirunamchandran, *Molecular Quantum Electodynamics* (Courier Dover, Mineola, NY, 1998).

[2] S.-M. Hu, H. Pan, C.-F. Cheng, Y. R. Sun, X.-F. Li, J. Wang, A. Campargue, and A.-W. Liu, Astrophys. J. **749,** 76 (2012).

[3] S. Tojo, M. Hasuo, and T. Fujimoto, Phys. Rev. Lett. **92,** 053001 (2004).

[4] A. M. Kern and O. J. F. Martin, Phys. Rev. A **85,** 022501 (2012).

[5] A. M. Kern and O. J. F. Martin, Nano Lett. **11,** 482 (2011).

[6] V. V. Klimov and V. S. Letokhov, Phys. Rev. A **54,** 4408 (1996).

[7] V. S. Letokhov and V. G. Minogin, *Laser Control of Atoms and Molecules* (Oxford University Press, New York, 2007).

[8] C. Cohen-Tannoudji and D. Gury-Odelin, *Advances in Atomic Physics: An Overview* (World Scientific, Singapore, 2011).

[9] S. Haroche and J.-M. Raimond, *Exploring the Quantum: Atoms, Cavities, and Photons* (Oxford University Press, New York, 2006).

[10] R. Loudon, *The Quantum Theory of Light* (Oxford Science, New York, 2000), 3rd ed.

[11] L. Allen and J. Eberley, *Optical Resonance and Two-Level Atoms* (Dover, Mineola, NY, 1987).

[12] C. Cohen-Tanoudji, B. Diu, and F. Laloe, *Quantum Mechanics* (Wiley Interscience, Paris, 1977), Vol. II.

[13] L. Allen, M. W. Beijersbergen, R. J. C. Spreeuw, and J. P. Woerdman, Phys. Rev. A **45,** 8185 (1992).

[14] J. E. Curtis and D. G. Grier, Phys. Rev. Lett. **90,** 133901 (2003).

[15] L. Allen, S. M. Barnett, and M. J. Padgett, *Optical Angular Momentum* (IOP, Bristol, England, 2003).

[16] *Structured Light and Its Applications: An Introduction to Phase-Structured Beams and Nanoscale Optical Forces*, edited by D. L. Andrews (Academic, Burlington, MA, 2008).

[17] *The Angular Momentum of Light*, edited by D. L. Andrews and M. Babiker (Cambridge University Press, Cambridge, England, 2012).

[18] V. E. Lembessis, D. Ellinas, and M. Babiker, Phys. Rev. A **84,** 043422 (2011).

[19] J. W. R. Tabosa and D. V. Petrov, Phys. Rev. Lett. **83,** 4967 (1999).

[20] M. S. Bigelow, P. Zerom, and R. W. Boyd, Phys. Rev. Lett. **92,** 083902 (2004).

[21] A. V. Bezverbny, V. G. Niz'ev, and A. M. Tumaikin, Quantum Electron. **34,** 685 (2004).

[22] A. Alexanderscu, E. Di Fabrizio, and D. Cojoc, J. Opt. B **7,** 87 (2005).

[23] W. Zheng-Ling and Y. Jiang-Ping, Chin. Phys. Lett. **22,** 1386 (2005).

[24] M. Babiker, W. L. Power, and L. Allen, Phys. Rev. Lett. **73,** 1239 (1994).

[25] M. Babiker, C. R. Bennett, D. L. Andrews, and L. C. Dávila Romero, Phys. Rev. Lett. **89,** 143601 (2002).

[26] A. R. Carter, M. Babiker, M. Al-Amri, and D. L. Andrews, Phys. Rev. A **72,** 043407 (2005); A. R. Carter, M. Babiker, M. Al-Amri, and D. L. Andrews, Phys. Rev. A **73,** 021401 (2006).

[27] R. Fickler, R. Lapkiewicz, W. N. Plick, M. Krenn, C. Schaeff, S. Ramelow, and A. Zeilinger, Science **338,** 640 (2012).

[28] M. F. Andersen, C. Ryu, P. Cladé, V. Natarajan, A. Vaziri, K. Helmerson, and W. D. Phillips, Phys. Rev. Lett. **97,** 170406 (2006).

[29] A. Ramanathan, K. C. Wright, S. R. Muniz, M. Zelan, W. T. Hill III, C. J. Lobb, K. Helmerson, W. D. Phillips, and G. K. Campbell, Phys. Rev. Lett. **106,** 130401 (2011).

[30] B. T. Seaman, M. Krämer, D. Z. Anderson, and M. J. Holland, Phys. Rev. A **75,** 023615 (2007).

[31] R. A. Pepino, J. Cooper, D. Z. Anderson, and M. J. Holland, Phys. Rev. Lett. **103,** 140405 (2009).

[32] V. E. Lembessis, S. Al-Awfi, M. Babiker, and D. L. Andrews, J. Opt. **13,** 064002 (2011).

[33] P. S. Tan, X.-C. Yuan, J. Lin, Q. Wang, T. Mei, R. E. Burge, and G. G. Mu, Appl. Phys. Lett. **92,** 111108 (2008).